

Articles

Hyperbolic Reaction-Diffusion Equation for a Reversible Brusselator: Solution by a Spectral Method

Il-Hie Lee, Kwang-Yon Kim, and Ung-In Cho*

Department of Chemistry, Yonsei University, Seoul 120-749, Korea

Received October 24, 1998

Stability characteristics of hyperbolic reaction-diffusion equations with a reversible Brusselator model are investigated as an extension of the previous work. Intensive stability analysis is performed for three important parameters, N_{rd} , β and D_x , where N_{rd} is the reaction-diffusion number which is a measure of hyperbolicity, β is a measure of reversibility of autocatalytic reaction and D_x is a diffusion coefficient of intermediate X . Especially, the dependence on N_{rd} of stability exhibits some interesting features, such as hyperbolicity in the small N_{rd} region and parabolicity in the large N_{rd} region. The hyperbolic reaction-diffusion equations are solved numerically by a spectral method which is modified and adjusted to hyperbolic partial differential equations. The numerical method gives good accuracy and efficiency even in a stiff region in the case of small N_{rd} , and it can be extended to a two-dimensional system. Four types of solution, spatially homogeneous, spatially oscillatory, spatio-temporally oscillatory and chaotic can be obtained. Entropy productions for reaction are also calculated to get some crucial information related to the bifurcation of the system. At the bifurcation point, entropy production changes discontinuously and it shows that different structures of the system have different modes in the dissipative process required to maintain the structure of the system. But it appears that magnitude of entropy production in each structure give no important information related for states of system itself.

Introduction

Reaction-Diffusion systems have been studied extensively as a prototype of dissipative structure.¹ Chemical waves and patterns formed by the nonlinear combination of reaction and diffusion have the common features of pattern formation in nature. The evolution equations for chemical waves and patterns are a set of partial differential equations (PDEs) composed of reaction and diffusion parts. In describing diffusion phenomena, Ficks' law has conventionally been used, and it leads to parabolic PDEs. But the parabolic PDEs are inadequate for describing wave phenomena because the wave suggested by the parabolic equations propagates in infinite speed. The features of parabolic equations make themselves undesirable to describe wave phenomena. The inadequacy of parabolic equations was pointed out and the replacement of hyperbolic ones was suggested by previous researchers. In the previous studies^{2,3} it was shown that the inadequacy of the parabolic type can be overcome by the hyperbolic one. This work is on an extension of the previous studies. The hyperbolic equation has two main features which make it worthwhile using in the description of a reaction-diffusion system. One is that it gives a general and exact description of diffusion phenomena. Of course, it is more difficult to handle hyperbolic equations than parabolic ones, and the former give a fair approximation in general situations. However, the difficulty to solve hyperbolic equations can be compensated by their ability to give an exact descrip-

tion of diffusion phenomena and its thermodynamic consistency if diffusion fluxes are defined as nonlinear functions of diffusion forces. Another feature is that the hyperbolic system has distinct stability characteristics generalized from the parabolic one, because one can find new solutions that cannot exist in the parabolic system. The hyperbolic equations give more insight for natural pattern formations with the Turing instability⁴ than the parabolic equations.

In this work, stability characteristics and various features of solutions which occurs in the hyperbolic system will be examined in detail. A reversible Brusselator will be used as a reaction model, and linear stability analysis will be performed to investigate how stability characteristics change as hyperbolicity in the diffusion process increases. In some representative regions numerical solutions will be shown. Entropy production is another subject studied in the present work. Dissipative structures such as chemical oscillations, waves, and stationary geometric patterns maintain their structures at the cost of the dissipation of energy supplied from the surroundings and the production of entropy. Since the entropy production is a direct measure of the dissipative process occurring in system, it may give some information about the modes of dissipative structures. There have been studies made to see if the entropy may provide a clue for evolutionary principle of structures appearing in a nonequilibrium state.⁵⁻¹⁰ These studies have been focused mainly on chemically oscillating systems and the common results are that entropy productions of dissipative structures have dif-

ferent values from those in steady uniform states and show discontinuous changes in transition from the steady state to a dissipative structure. Entropy productions for the reaction-diffusion system will be calculated and compared with previous results of the homogeneous system evolving in time. A spectral method has been used to obtain numerical solutions for hyperbolic PDEs. It was observed that the spectral method¹¹⁻¹³ could be easily adapted to hyperbolic PDEs. The method is accurate and efficient compared with the conventional finite difference or finite element method for hyperbolic PDEs. Also, it can be extended to a higher dimensional system more easily than the conventional methods.

Hyperbolic Reaction-Diffusion Equations

The hyperbolic reaction-diffusion equations are as follows:

$$\partial_t c_i = -\nabla \cdot \mathbf{J}_i + \Lambda_i(c), \quad (1a)$$

$$\partial_t \mathbf{J}_i = -(\rho k_B T / m_i) \nabla c_i - \sum_j L_{ij} \mathbf{J}_j \quad (1b)$$

It is assumed that the fluid is incompressible with no convection flow and homogeneous in temperature. Transport of all species in this system is due to diffusion only. With these assumptions all dissipative processes that occur in the system are those due to the reactions and the diffusion. We denote the mass fraction for species i by c_i and the diffusion flux by \mathbf{J}_i . The $\Lambda_i(\mathbf{c})$ is the reaction rate term, m_i is the mass of species i , is the mass density, and L_{ij} are phenomenological coefficients.

The reaction model is the reversible Brusselator.¹⁴



In this model it is assumed that the concentration of the reactants and products (A , B , D and E) are kept constant, while intermediate, X and Y can be changed freely. All processes are reversible. Since the fluxes of two intermediate, \mathbf{J}_X and \mathbf{J}_Y are independent variables, the dimension of the system is four. As the dimensions are larger than three, one can expect more interesting results such as chaotic behaviors besides well-organized dissipative structures.

Now the evolution equations for our system are given in scaled forms¹⁴ as follows:

$$\frac{\partial X}{\partial \tau} = -\frac{\partial u}{\partial \xi} + A - \alpha X - BX + YD + X^2 Y - \beta X^3 - X + E, \quad (3a)$$

$$\frac{\partial Y}{\partial \tau} = -\frac{\partial v}{\partial \xi} + BX - YD - X^2 Y + \beta X^3, \quad (3b)$$

$$\frac{\partial u}{\partial \tau} = -N_{rd} \left(D_X \frac{\partial X}{\partial \xi} + fu \right), \quad (3c)$$

$$\frac{\partial v}{\partial \tau} = -N_{rd} \left(D_Y \frac{\partial Y}{\partial \xi} + \frac{1}{f} v \right). \quad (3d)$$

All of parameters are scaled as follows :

$$\tau = k_4 t, \quad \xi = r/L, \quad X = \left(\frac{k_3}{k_4} \right)^{\frac{1}{2}} \rho_X, \quad Y = \left(\frac{k_3}{k_4} \right)^{\frac{1}{2}} \rho_Y,$$

$$A = \frac{k_1}{k_4} \left(\frac{k_3}{k_4} \right)^{\frac{1}{2}} \rho_A, \quad B = \left(\frac{k_2}{k_4} \right) \rho_B,$$

$$D = \left(\frac{k_2}{k_4} \right) \rho_D, \quad E = \frac{k_4}{k_4} \left(\frac{k_3}{k_4} \right)^{\frac{1}{2}} \rho_E, \quad u = \frac{1}{L k_4} \left(\frac{k_3}{k_4} \right)^{\frac{1}{2}} J_X$$

$$v = \frac{1}{L k_4} \left(\frac{k_3}{k_4} \right)^{\frac{1}{2}} J_Y, \quad N_{rd} = \frac{k_B T / (m_X m_Y)^{\frac{1}{2}}}{k_4 (\bar{D}_X \bar{D}_Y)^{\frac{1}{2}}}, \quad f = \left(\frac{m_Y \bar{D}_Y}{m_X \bar{D}_X} \right)^{\frac{1}{2}},$$

$$D_X = \frac{f \bar{D}_X}{L^2 k_4}, \quad D_Y = \frac{f \bar{D}_Y}{L^2 k_4}, \quad \alpha = k_{-1}/k_4, \quad \beta = k_{-3}/k_3$$

where k_i and $k_{-i}(i=1-4)$ are the forward and reverse rate coefficients, and L is the linear dimension of the system. \bar{D}_i is the diffusion coefficient of species i defined by $\bar{D}_i = (k_B T / m_i) / L_{ii}$, $i=X$ and Y .

The focus will be on three parameters, N_{rd} , β , and D_X which have considerable physical meaning and critically affects the stability of the system. The N_{rd} is called the reaction-diffusion number, a measure of hyperbolicity of the diffusion process. The β is the measure of reversibility of the autocatalytic process; if $\beta=0$, it then corresponds to only forward reaction, and if $\beta \rightarrow \infty$ it corresponds to the reverse reaction in (2c). The value of D_X will be selected to give the desired ratio of the diffusion coefficients of X and Y .

Only a contribution of the reaction part to the entropy production will be considered because the magnitude of the entropy production due to diffusion is very small when compared with one due to the reaction. The rate of entropy production per unit volume due to the reaction is given as follows

$$\bar{\sigma}_r = k_B \sum_i (\Lambda_i^{(+)} - \Lambda_i^{(-)}) \ln(\Lambda_i^{(+)} - \Lambda_i^{(-)}). \quad (4)$$

This equation can be written as

$$\bar{\sigma}_r = (A - \alpha X) \ln(A / \alpha X) + (BX - YD) \ln(BX / YD) + (X^2 Y - \beta X^3) \ln(Y / \beta X) + (X - E) \ln(X / E) \quad (5)$$

and in scaled form as

$$\sigma_r = k_B k_4 \left(\frac{k_4}{k_3} \right)^{\frac{1}{2}} \bar{\sigma}_r. \quad (6a)$$

$$P_{chem} = \int \sigma_r dV \quad (6b)$$

Linear Stability Analysis²

Eqs. (3a)-(3d) has a steady state with

$$X_s = \frac{A+E}{1+\alpha}, \quad (7a)$$

$$Y_s = \frac{X_2(B + \beta X_s^2)}{D + X_s^2}, \quad (7b)$$

$$u_s = 0, \quad (7c)$$

$$v_s = 0. \quad (7d)$$

$$x = \sum_m^{\infty} \exp(\omega_m \tau) p_m \sin(\pi m \xi), \quad (10a)$$

$$y = \sum_m^{\infty} \exp(\omega_m \tau) q_m \sin(\pi m \xi), \quad (10b)$$

$$u_x = \sum_m^{\infty} \exp(\omega_m \tau) r_m \cos(\pi m \xi), \quad (10c)$$

$$u_y = \sum_m^{\infty} \exp(\omega_m \tau) s_m \cos(\pi m \xi), \quad (10d)$$

These values correspond to spatially homogeneous solutions of Eqs. (3a)-(3d). The stability of the stationary steady state is determined by the behavior of small perturbation, x and y defined by

$$x = X - X_s, \quad (8a)$$

$$y = Y - Y_s. \quad (8b)$$

Assuming that the magnitude of x and y is small, a set of linearized equations for x and y can be obtained as follows :

$$\frac{\partial x}{\partial \tau} = -\frac{\partial u}{\partial \xi} - (\gamma + \phi)x + \theta y, \quad (9a)$$

$$\frac{\partial y}{\partial \tau} = -\frac{\partial v}{\partial \xi} + \phi x - \theta y, \quad (9b)$$

$$\frac{\partial u_x}{\partial \tau} = -\varepsilon_x \frac{\partial x}{\partial \xi} - l_x u_x, \quad (9c)$$

$$\frac{\partial u_y}{\partial \tau} = -\varepsilon_y \frac{\partial y}{\partial \xi} - l_y u_y, \quad (9d)$$

where

$$\phi = B + \beta \frac{M^2}{\gamma^2} + 2M^2 \frac{\beta D - B}{D\gamma^2 + M^2},$$

$$\theta = D + \frac{M^2}{\gamma^2}, \quad \varepsilon_x = N_{rd} D_X, \quad \varepsilon_y = N_{rd} D_Y,$$

$$l_x = N_{rd} f, \quad l_y = N_{rd} f', \quad M = A + E, \quad \gamma = 1 + \alpha.$$

Using the boundary conditions $x=y=0$ at $\xi=0$ and 1, solutions for Eq. (9) can be expected as :

Then the following characteristic equation can be obtained:

$$\omega^4 + P\omega^3 + Q\omega^2 + R\omega + S = 0, \quad (11)$$

where

$$P = \gamma + \theta + \psi + l_x + l_y, \quad (12a)$$

$$Q = (\gamma + \theta + \psi)(l_x + l_y) + \gamma\theta + l_x l_y + \pi^2(\varepsilon_x + \varepsilon_y)m^2, \quad (12b)$$

$$R = \gamma\theta(l_x + l_y) + (\gamma + \theta + \psi)l_x l_y + \pi^2[\varepsilon_x(\theta + l_y) + \varepsilon_y(\gamma + \theta + l_x)]m^2, \quad (12c)$$

$$S = \gamma\theta l_x l_y + \pi^2[\theta \varepsilon_x l_x + (\gamma + \psi)\varepsilon_y l_y]m^2 + \pi^4 \varepsilon_x \varepsilon_y m^4, \quad (12d)$$

The conditions for all the roots of the aforementioned equation to have nonpositive real parts are the following conditions due to Lienard-Chipart¹⁵ :

$$P > 0, \quad (13a)$$

$$Q > 0, \quad (13b)$$

$$S > 0, \quad (13c)$$

$$PQR - R^2 - P^2S > 0. \quad (13d)$$

When all four conditions above are not satisfied, the system will be unstable.

The stability conditions in (13) give rise to a relation of B to parameters such as N_{rd} , β , and D_X . These stability conditions are established after B is plotted in terms of m with given parameters. For small values of B , stationary steady states are maintained. As some critical concentration B_c of B exceeded, the steady state becomes unstable and thus various spatially oscillatory or chaotic patterns in solution Eq. (9) appear, depending on the conditions (13). There exist four critical values of B . The first two values from conditions (13a) and (13b) are larger than those from the third (condition (13c)) and fourth (condition (13d)) for all conditions of interest. Thus, the third and fourth critical values, which will be denoted as B_{c3} and B_{c4} , respectively, are the main objects of discussion. Parameter dependence of stability within the limit of N_{rd} , β , D_X as shown from Figure 1 to 4 will be discussed. In the figures, the broken and solid lines

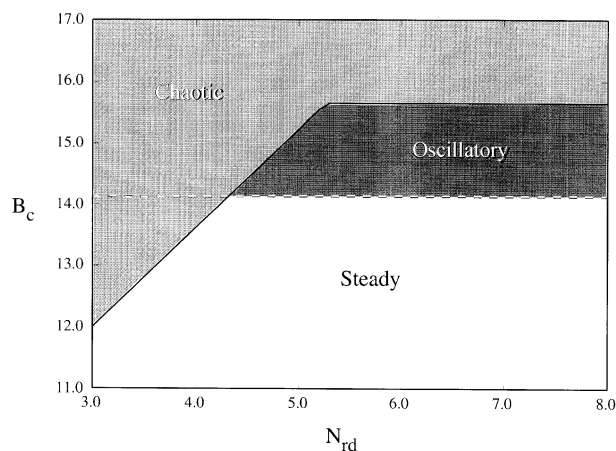


Figure 1. The stability analysis depending on N_{rd} . $\beta=0.5$, $D_X=0.0016$. (Solid line: B_{c4} ; Broken line: B_{c3})

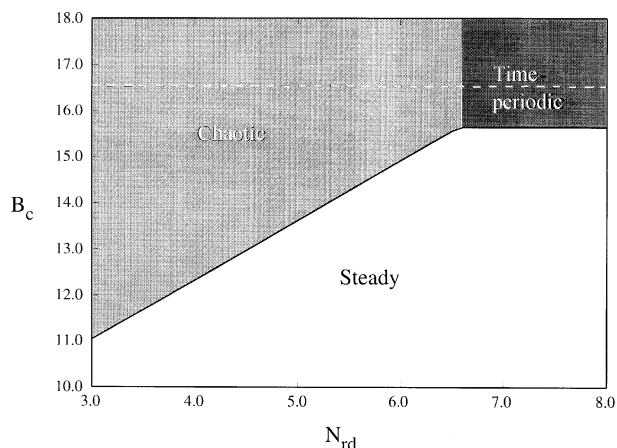


Figure 2. The stability analysis depending on N_{rd} . $\beta=0.5$, $D_X=0.0025$. (Solid line: B_{c4} ; Broken line: B_{c3})

will correspond to B_{c3} and B_{c4} , respectively. Generally speaking, as B is increased from the region of stable solution while other parameters are fixed, a chaotic solution appears at the intersection with B_{c4} critical value while an oscillatory solution appears on crossing B_{c3} . It should be noted that when crossing B_{c3} occurs ahead of B_{c4} an oscillatory solution appears for a short time until B_{c4} is reached. However crossing B_{c4} occurs ahead of B_{c3} , a chaotic solution is maintained to even if B_{c3} is crossed.

Stability dependences on N_{rd} , a measure of hyperbolicity, are shown in Figure 1 and 2. In the figures, B_{c3} does not depend on N_{rd} , but B_{c4} has two distinct dependences. Approximately as shown in Figure 1 and 2, B_{c4} does not depend on N_{rd} in the large value region, while in the small value region up to some value of N_{rd} , B_{c4} increases linearly on N_{rd} increments. Thus B_{c3} can be located on either below or above B_{c4} . In Figure 1, above B_{c4} the chaotic solution is shown regardless of the relative locations of B_{c3} ; however, in the narrow region between B_{c3} and B_{c4} , an oscillatory solution appears. In contrast, in Figure 2 where B_{c3} is above B_{c4} in whole range of N_{rd} , a little peculiar pattern is shown. Above B_{c4} where the linear dependence on N_{rd} is shown, the

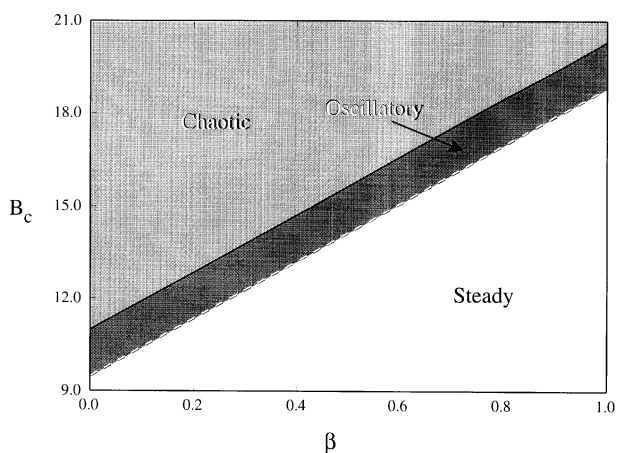


Figure 3. The stability analysis depending on β . $N_{rd}=6.0$, $D_X=0.0016$. (Solid line: B_{c4} ; Broken line: B_{c3})

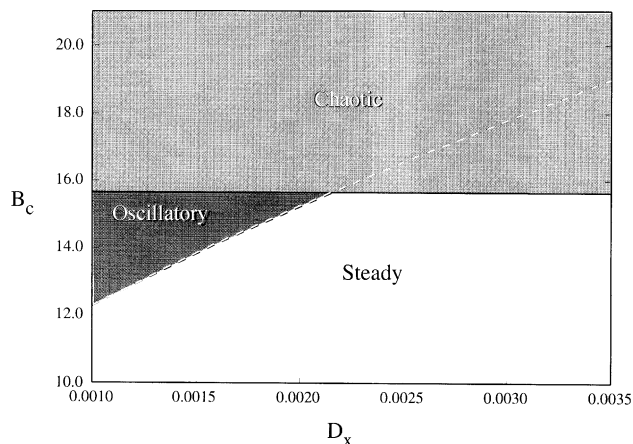


Figure 4. The stability analysis depending on D_X . $N_{rd}=6.0$, $\beta=0.5$. (Solid line: B_{c4} ; Broken line: B_{c3})

chaotic solution appears as expected. But above B_{c4} in which there is a nondependence of N_{rd} , a time-periodic pattern appears. Thus two regions with N_{rd} dependence on B_{c4} will be distinguished. We will call the region of the non-dependence on N_{rd} the parabolic region and the region of the linear dependence on N_{rd} the hyperbolic region. It may be interpreted that as N_{rd} increases to a certain value, the hyperbolic differential equations effectively become parabolic equations.

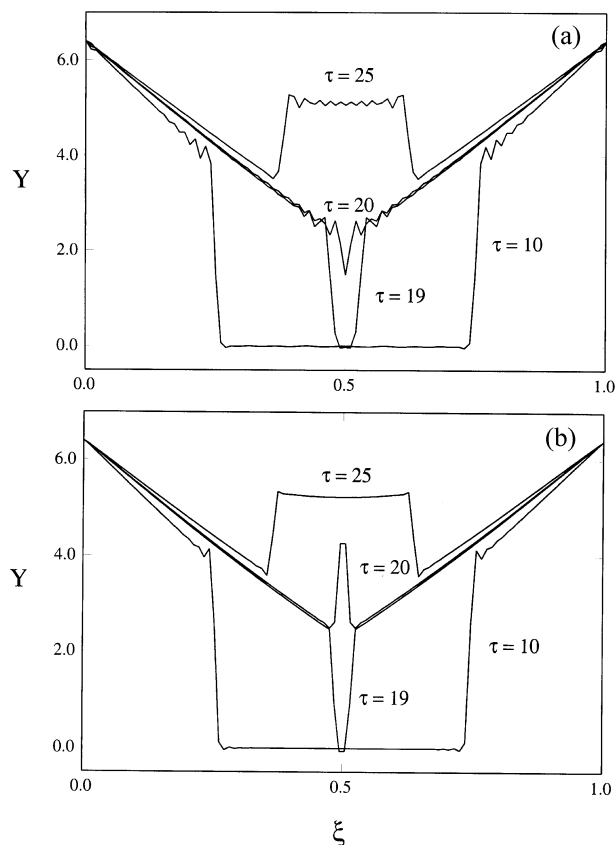


Figure 5. The comparison of (a) finite difference method and (b) spectral method at various scaled τ . $B=14.0$, $N_{rd}=0.1$, $D_X=0.0016$, $\beta=0.5$.

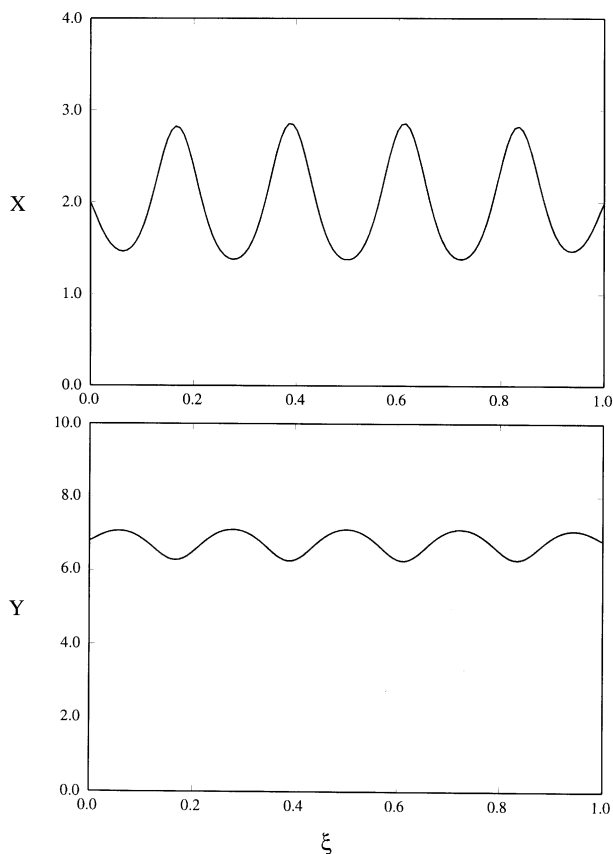


Figure 6. The steady oscillatory pattern at the scaled time $\tau=1000$. $B=13.0$, $N_{rd}=6.0$, $D_X=0.0016$.

Dependence on β , a measure of reversibility of (2c), is rather simple for both B_{c3} and B_{c4} as shown in Figure 3. They linearly depend on β with $B_{c3} < B_{c4}$, which means that above B_{c4} a chaotic solution appears and between B_{c3} and B_{c4} an oscillatory solution is expected. It is worthwhile to note that since the range of B where the steady state is stable increases as the reversibility of (2c) increases, there will be no dissipative or chaotic structure in the autocatalytic process in the limit of completely reversible reactions.

The stability dependence on D_x is depicted in Figure 4. As D_x increases, B_{c3} is increased while B_{c4} is decreased with much lower slope. Thus, they intersect at a certain D_x . In the case of a smaller value of D_x , the stability crossing of the B_{c3} occurs ahead of B_{c4} , whereas in the case of a larger value of D_x the stability crossing of B_{c4} occurs ahead of B_{c3} . As noted previously, a chaotic solution appears on crossing B_{c4} , but an oscillatory pattern shows up only when $B_{c3} < B_{c4}$ in the case of smaller values of D_x .

Numerical Results and Discussion

For numerical simulations, spectral methods¹¹⁻¹³ are modified and adapted to hyperbolic reaction-diffusion equations. The Fourier collocation method is used to have satisfactory solutions for Eqs. (3a)-(3d). In computation both accuracy in solutions and numerical efficiency are required even when stiff solutions occur in the case of small N_{rd} . To compare the

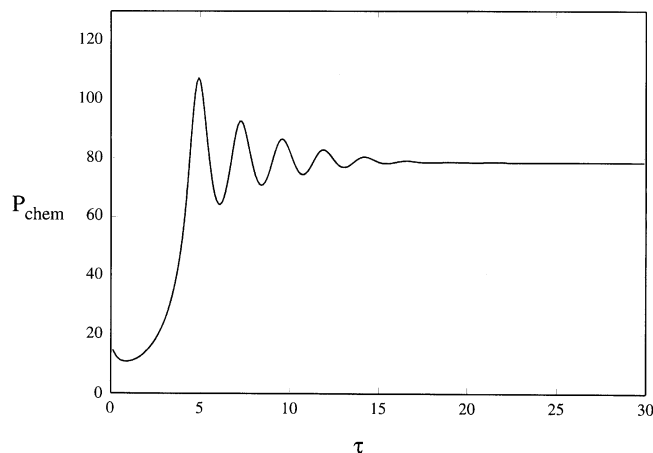


Figure 7. The time evolution of entropy production in steady oscillatory pattern.

spectral method in this work with the finite difference method, calculations were performed in which only the diffusion term is taken into consideration by excluding reaction parts in Eqs. (3a)-(3d). The numerical solutions are obtained for $N_{rd}=0.1$; a sharp wave-front because of a relatively large diffusion velocity was expected. As shown in Figure 5, the spectral method exhibited a far better solution in sharpness and smoothness than the finite difference method (FDM) by the MOLCH routine in IMSL. Especially in the process which two wave-fronts meet and propagate in reverse direc-

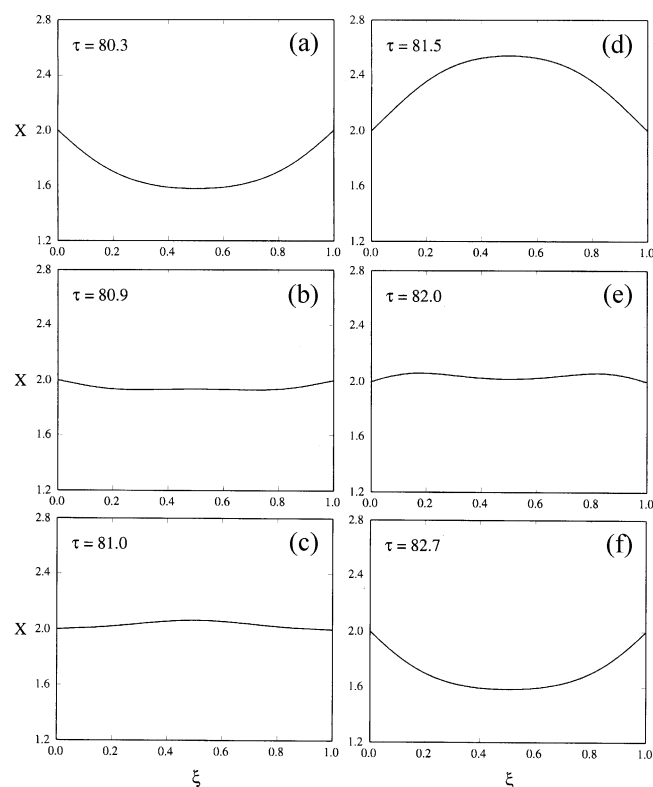


Figure 8. The periodic oscillatory pattern at the scaled time (a) $\tau=80.3$, (b) $\tau=80.9$, (c) $\tau=81.0$, (d) $\tau=81.5$, (e) $\tau=82.0$, (f) $\tau=82.7$. $B=16.0$, $N_{rd}=7.5$, $D_X=0.0025$.

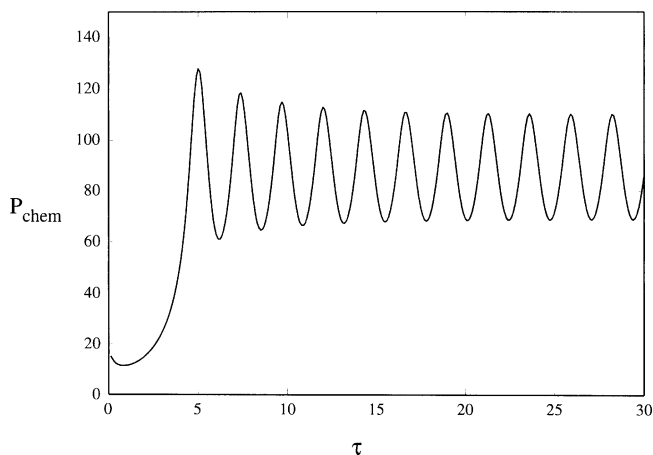


Figure 9. The time evolution of entropy production in periodic oscillatory pattern.

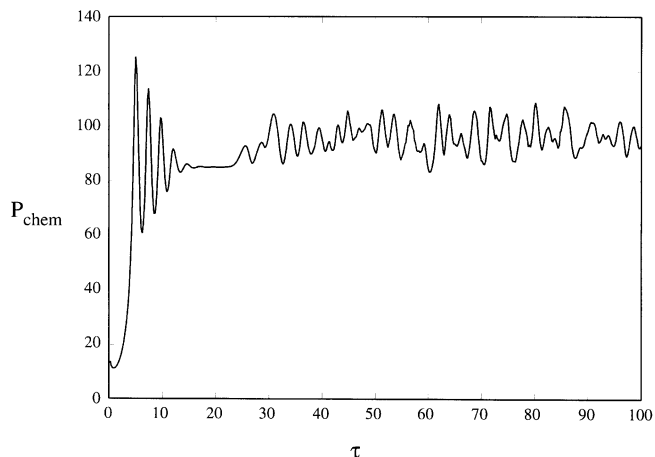


Figure 11. The time evolution of entropy production in unstable chaotic pattern.

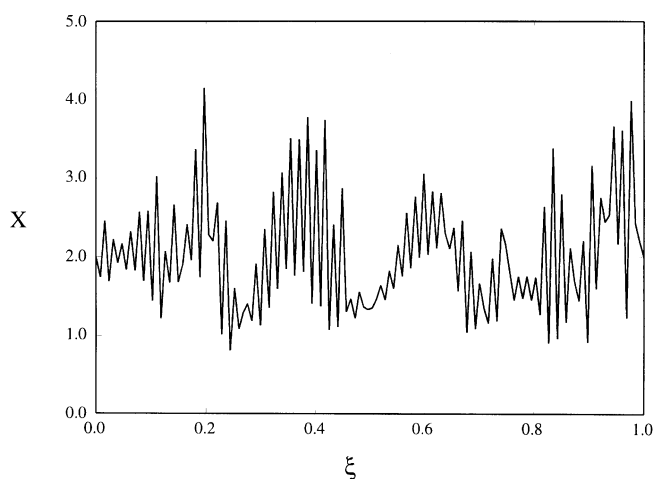


Figure 10. The chaotic pattern at the scaled time $\tau=500$. $B=16.0$, $N_d=4.0$, $D_x=0.0016$.

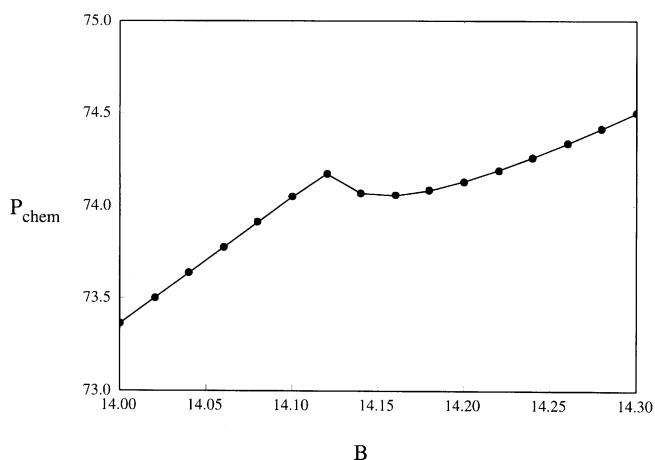


Figure 12. The change of entropy production at transition from thermodynamic branch to dissipative structure.

tions, the spectral method gives excellent results. It can be concluded then that the spectral method expresses itself far better even for very stiff solutions in space. Furthermore, with numerical efficiency with the same mesh size, the spectral method consumes less than half the time compared with the FDM and the incremental rate of computation time with the expansion of mesh size is far lower with the spectral method. This will lead to a crucial advantage in extending the method to a case of a higher dimension in space.

Four types of solutions, spatially homogeneous, spatially oscillatory (Fig. 6), spatiotemporally oscillatory (Fig. 8) and chaotic (Fig. 10), have been obtained. Entropy productions are also calculated to get some clues for the dissipative process occurring in the system, specifically to investigate how it changes in the course of a pattern formation. The spatially homogeneous solutions can be obtained for parameter sets of steady regions such as indicated in Figure 1-4. As shown in Figure 6 the spatially oscillatory solution exhibits a stable pattern for parameter sets of oscillatory regions as pointed in Figure 1-4 after an adequate amount of time. The pattern can be selected by setting suitable values for parameters. For

example, a half wave number of patterns can be controlled by changing D_x . Figure 7 shows the time evolution of entropy production corresponding to this pattern. After some fluctuations the entropy production converges to a stable value. The spatio-temporally oscillatory solutions appear in a rather peculiar set of parameters shown in Figure 2 which is expressed as time-periodic. It looks like a vertically oscillating rope seen transversally. In this situation a pattern control is not possible, and only one pattern with a half wave number can exist. In Figure 9 the entropy production evolves periodically in time. Lastly, as the value of B increases up to the chaotic region, the chaotic pattern or chemical turbulence occurs as depicted in Figure 10. The chaotic pattern does not appear instantly from the initial condition near the bifurcation point; it's very slow to appear. But in the range sufficiently far from B_{c4} it appears without delay. As shown in Figure 11 the entropy production seems to evolve with a periodical pattern in induction period, but after some time to fluctuate disorderly.

The variation of entropy production with regard to B is calculated to investigate how it changes when the state of the

system changes. Figure 12 shows that entropy production changes discontinuously at the bifurcation point. It means that two states have different modes of energy dissipation to maintain their structures. In the dissipative structure the system has a lower entropy production value than a homogeneous structure. But it cannot be definitely stated that dissipative structures have a lower entropy production than homogeneous steady states for general cases. It appears that the value of entropy production itself does not give any information about the determination of states. The transition is second order, but there is something uncertain to conclude about the transition to a dissipative structure in a reaction-diffusion system is second-order because the variation of entropy production is small in its scale. But when calculated in a two dimensional system, it becomes certain. On the other hand, in the case of a transition to a chaotic state the system has a higher value of entropy production than a homogeneous one, and an abrupt change of entropy production is found at the transition point between two states. It seems that the system consumes more energy to maintain the homogeneous state than the dissipative structure.

To describe real chemical wave phenomena and to get a more exact definition of diffusion fluxes, hyperbolic equations are required. As mentioned earlier, it has already been shown that the hyperbolic system has very different stability characteristics from the parabolic system. When it is investigated how the stability depends on hyperbolicity, there are two regions having different stability characteristics, namely hyperbolic and parabolic regions. In the hyperbolic region the range in which dissipative structures occur is narrow and chaotic states appear in a wide range. In the parabolic region chaotic states may or may not occur depending on the conditions of the system such as diffusion coefficients. It is remarkable that chaotic structures occur in a wide range of parameters and may be general phenomena far from equilibrium. It appears that it is a necessary balance between force and flux for the dissipative structure to emerge, and when the balance breaks down, two extreme structures, such as a homogeneous or chaotic pattern may appear. Since the

entropy production is a direct measure of the dissipative process occurring in a system, it is calculated in various states, and it seems to reflect the mode of dissipation in a system. In a transitional state the entropy production shows a discontinuous change and it originates from two different states which have different modes of energy dissipation. But it does not give any direction to the evolution of a system, and its only worth seems to be as a measure of the dissipation process under consideration.

Acknowledgement. This work was supported by Special Basic Research from KOSEF (95-05-00-15) and Academic Research Fund from Yonsei University. (93-109).

References

1. *Oscillations and Traveling Waves in Chemical Systems*; Field, R. J.; Burger, M. Eds.; Wiley: New York, **1985**.
2. Cho, U. I.; Eu, B. C. *Physica D* **1993**, *68*, 351.
3. (a) Al-Ghoul, M.; Eu, B. C. *Physica D* **1996**, *90*, 119. (b) Al-Ghoul, M.; Eu B. C. *Physica D* **1996**, *97*, 531.
4. Turing, A. *Phil. Trans. R. Soc. London Ser. B* **1952**, *327*, 37.
5. Ali, J.; Eu, B. C. *J. Chem. Phys.* **1984**, *81*, 4401.
6. Mansson, B. A. G. *Z. Naturforsch. Teil A* **1985**, *40*, 877.
7. Dutt, A. L. *J. Chem. Phys.* **1987**, *86*, 3959.
8. Irvin, B. R.; Ross, J. *J. Chem. Phys.* **1988**, *89*, 1064.
9. Yoshida, N. *J. Chem. Phys.* **1990**, *92*, 2593.
10. Dutt, A. K.; Bhattacharya, D. K.; Eu, B. C. *J. Chem. Phys.* **1990**, *93*, 7929.
11. Gottlieb D.; Orszag, S. A. *Numerical Analysis of Spectral Methods : Theory and Applications*; Society for Industrial and Applied Mathematics: Philadelphia, **1977**.
12. Canuto, C.; Hussaini, M. Y.; Quarteroni, A.; Zang, T. A. *Spectral Methods in Fluid Dynamics*; Springer-Verlag: New York, **1988**.
13. Hussaini, M. Y.; Zang, T. A. *Ann. Rev. Fluid Mech.* **1987**, *19*, 339.
14. Nicolis, G.; Prigogine, I. *Self-Organization in Nonequilibrium Thermodynamics*; North-Holland: Amsterdam, **1962**.
15. Grantmacher, F. R.; *Theorie des Matrices*; Dunod: Paris, Vol 2.